FINITE ELEMENT ANALYSIS ON THE NONLINEAR BEHAVIOR OF RC SHEAR WALL WITH REGULAR OPENINGS INFLUENCED BY HIGH-STRENGTH STEEL

Ika S. Nurahida[a], Bambang Piscesa[b*], Pujo Aji[b], Asdam Tambusay[b]

***Abstract**: This paper presented a nonlinear finite element analysis of lateral loading RC shear walls with regular openings using the 3D-NLFEA program. The RC shear walls model was generated from the available test results in the literature. To model the concrete under a complex stress state, a multi-surface plasticity model which combines compression failure surface with tension cut-off failure surface was used. The model was intended to look at the load-displacement relationship and the crack pattern between the model and the numerical model. In addition to the numerical model verification, parametric studies were carried out to investigate the use of high-strength steel (HSS) of the two different grades (Grades 100 and 120) to replace all the normal-strength steel (NSS) or only some of it. The parametric studies found that the shear wall with the NSS bar demonstrated higher stiffness and achieved higher lateral load with the lowest extent of damage (compared to the RC shear wall with the HSS bar). On the other hand, using the HSS bar resulted in lower stiffness, lower lateral load, and higher damage region, which was expected as more strain is required to yield the HSS bar.*

Keywords: *Multi-surface plasticity model, nonlinear finite element analysis, high-strength bar, stiffness, damage*

Submitted: 29 June 2022; Revised: 24 December 2022; Accepted: 24 December 2022

INTRODUCTION

The shear wall is one of the structural components designed to withstand lateral loads due to earthquakes and the axial forces of the structure. Based on research [1], the leading cause of failure of a building's structural system during an earthquake is the loss of the ability to withstand lateral loads. Therefore, shear walls are widely used to resist high-rise buildings' earthquake loads. One of the major concerns in designing shear walls is the presence of opening such as windows, emergency doors, elevators, corridors, mechanical and electrical conduits, and other functions. Openings in shear walls reduce the stiffness and generate stress concentration at the edges [2]. The structure's behavior may differ for a large shear wall opening [3]. In the worst scenario, the structural system may change [4][5].

On the other hand, as the material technology develops, the use of higher concrete compressive strength and higher yield strength for the reinforcing bar becomes attractive. Using these high-strength materials can significantly increase the design efficiency of the high-rise building. From [6], using high-strength materials can reduce the construction cost, structural element size, and possible rebar congestion and improve the building structures' quality. Other studies [7] also noted that combining HSS and NSS rebar in RC shear walls can increase the displacement capacity and provide excellent deformation ability compared to RC shear walls with only NSS rebar. In contrast with the finding in [7], using HSS as the shear reinforcement in RC beams can increase the crack width at service load levels.

The study of [8], which uses HSS rebar as the shear reinforcement in beams, can increase the width of cracks at service load levels and showed different failure behavior due to the development of flexural compression zones on structural members experiencing shear. In this study, using HSS as shear reinforcement met the limits of ACI 318-19 [9] but also showed shear stress failure when the yield strength of the shear reinforcement exceeded 600 MPa.

The material properties of the concrete and rebar used in earthquake-resistant RC will significantly affect the behavior of the structure [10]. The rebar material properties must be within the limits of applicable regulations to prevent structural failure [11]. To avoid this, ACI 318-19 [9] limits the use of reinforcing steel with a yield strength of 560 MPa (Grade 80) for flexural reinforcement, shear reinforcement, and torsion reinforcement. This limitation is due to high strength reinforcing steel resulting in higher shear and bond stresses when the load increases.

Developed countries such as America, New Zealand, and Japan have used high-strength rebar with a yield strength of up to 700 MPa for earthquake-resistant building structures. The use of reinforcing steel with a yield strength greater than 420 MPa (Grade 60) may be used if it complies with ASTM specifications, following ASTM specified in ACI 318-19 [9]. The National Institute of Standards and Technology issued a NIST [12] report which discusses the terms and conditions for using high-strength reinforcing steel in earthquake-resistant building structures. Based on this research, reinforcement with ASTM 706 [13] Grade 80 shows strength and deformation capacity like that of Grade 60 reinforcement. ACI Regulation [9] Article 18.2.6.1 states that the use of rebar with a quality of more than 420 MPa can be used for earthquake-resistant reinforced concrete structures is permitted if there was support from the experimental tests and detailed analysis. ASTM A615M-15 [14] contains specifications for carbon steel reinforcement with a quality of up to 690 MPa (Grade 100). The use of reinforcing steel with a yield strength of more than 420 MPa (Grade 60) can be used if the values for the strength parameters of the reinforcing steel were included. The use of HSS has advantages and disadvantages, as described above, so a combination of HSS and NSS is carried out to complement each other's strengths and weaknesses.

[a]Master Student in the Civil Engineering Department, Institut Teknologi Sepuluh Nopember, ITS Campus, Sukolilo, Surabaya 60111, Indonesia.
[b]Civil Engineering Department, Institut Teknologi Sepuluh Nopember, ITS Campus, Sukolilo, Surabaya 60111, Indonesia. Corresponding author email address: piscesa@ce.its.ac.id

RESEARCH SIGNIFICANCE

This paper investigates the nonlinear performance of RC shear walls with regular openings influenced by HSS. To verify the validity of the numerical model using 3D-NLFEA, the numerical model was confirmed with the existing experimental test for shear walls with openings built with normal-strength steel. After the numerical model can reasonably predict the behavior of the modelled shear wall, modification of the shear wall reinforcement using HSS and a combination of HSS and NSS were presented.

METHODOLOGY

The research methodology in this paper consisted of two stages. The first stage of this research was model verification. At this stage, the analysis is focused mainly on the result of the load-displacement relationships and the crack patterns. The second stage was the modification of the verified model to evaluate the effect of using HSS with two different grades (i.e., G100 [Grades 100] and G120 [Grades 120]) along with the combination of the HSS and NSS.

A. 3D-NLFEA MODEL VERIFICATION WITH EXISTING EXPERIMENTAL TEST

For verification purposes, the numerical model using 3D-NLFEA finite element package was verified with the current experimental work carried out by [15]. The experimental work in [15] consisted of a shear wall with an opening, and the reinforcement was classified as normal-strength steel (NSS). From [15], only one specimen with ID SW8 was investigated. Figure 1 shows the geometric configuration of the shear wall in mm. Figure 2 shows the reinforcement details. Table 1 and Table 2 show the material properties of the concrete and the reinforcing bar, respectively.

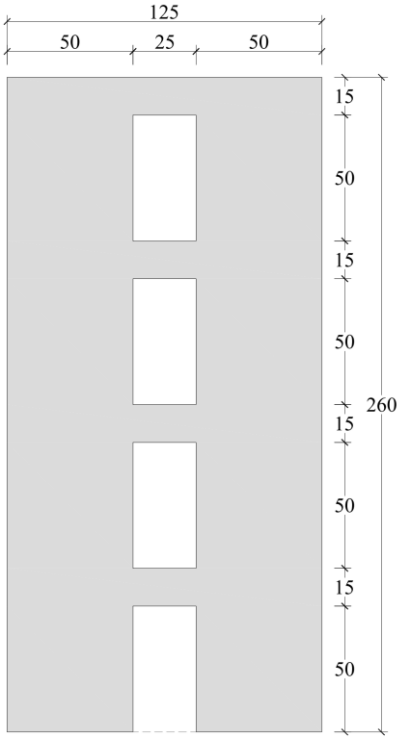

Figure 1 Geometric of the shear wall

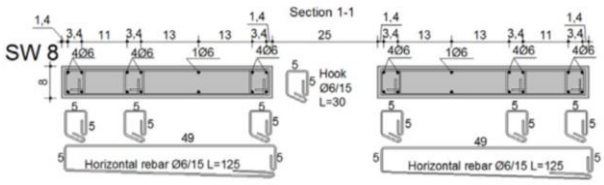

Figure 2 Rebar configuration [15]

Table 1 Material properties of the concrete

Average Compressive Strength (kN/mm^2)	Average Tensile Strength (kN/mm^2)	Compressive Strain	Modulus of Elasticity (kN/mm^2)
0.05	0.003	3.5%	34

Table 2 Tensile properties of the NSS

Diameter (mm)	Yield Strength (kN/mm^2)	Ultimate Strength (kN/mm^2)	Modulus of Elasticity (kN/mm^2)
6	0.386	0.551	200

The auxiliary program used to model the geometrical cross-section of the shear wall structure was SALOME 9.3.0. The model consists of solid elements consisting of concrete, a 25 mm thick steel plate, horizontal reinforcement, and vertical reinforcement. The steel plate was used as the accumulator plate. The experimental loading is considered seismic loading according to FEMA (2002), but in numerical modelling, it was assumed to be a monotonic loading with displacement control.

Figure 3 shows the loading assumption used in the numerical model. In Figure 3, the push and pull motion from the accumulator was assumed to be rigid, and at the top of the shear wall, a uniform distributed load with a total magnitude of 50 kN was added. The restraint in the shear wall model was assumed to be fixed in all directions (Figure 4d). The model has meshed with hexahedron type (eight-node hexahedral element), and the mesh size is 25 mm.

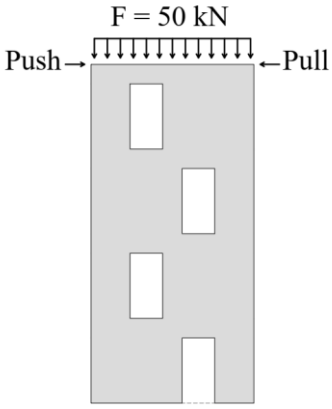

Figure 3 Loading assumption

The discretized geometry data was obtained through the SALOME 9.3.0 program, where the data was in the form of a ".dat" file which would then be inputted into excel and became the input file for the 3D-NLFEA program. The constitutive model used for concrete was the plasticity fracture concrete model, according to the research of [16]–[23]. While the constitutive rebar model used was bilinear stress-strain [5], [24].

Figure 4 shows the shear wall model in SALOME. Figure 4a shows the concrete model. Figure 4b shows the NSS bar configuration, and the rebars were shown to be red colored. Figure 4c shows the 100 mm thick accumulator plate model. Figure 4d shows the solid configuration and lastly, Figure 4e shows the discretion of the meshed model. The output results were obtained from the lateral load and the top displacement. These results would then be compared with the experimental results in [15].

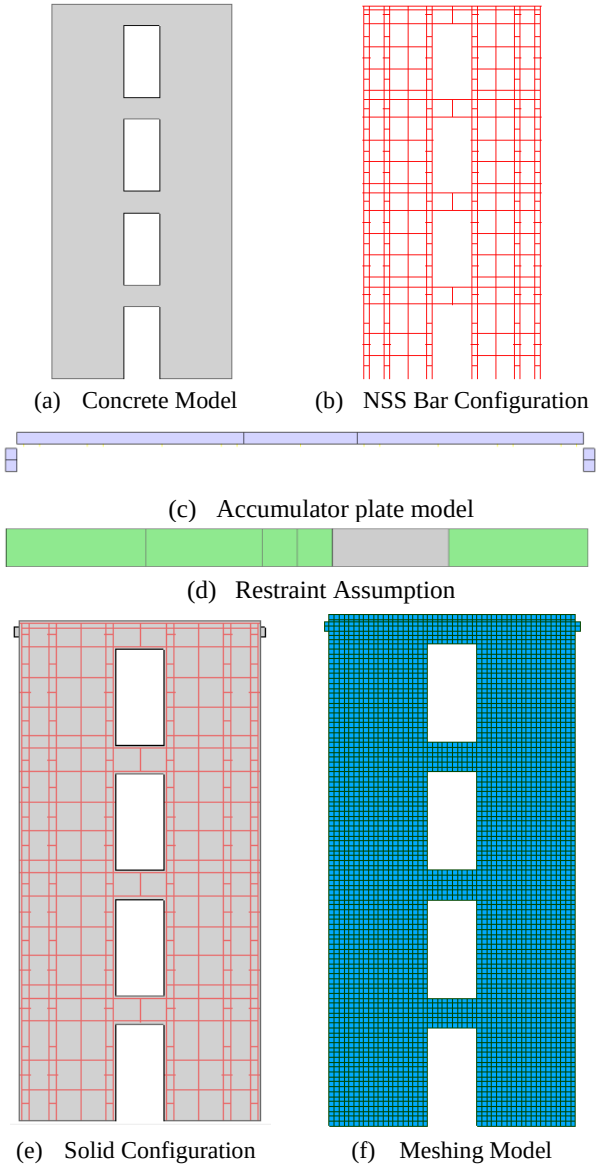

(a) Concrete Model (b) NSS Bar Configuration

(c) Accumulator plate model

(d) Restraint Assumption

(e) Solid Configuration (f) Meshing Model

Figure 4 Modeling shear wall in SALOME

The numerical model's accuracy was evaluated by investigating the lateral load covariance at each load level (elastic, post-yielding, ultimate, and failure), as shown in Table 3 and Figure 5. Table 3 shows the exact values obtained from the test result and the numerical model. As shown in Table 3, the mean ratio from the elastic to the ultimate stage was found to be 0.971, and the covariance is 1.02 %. The small number of covariance and mean values close to unity indicates that the numerical model using 3D-NLFEA was sufficiently accurate.

Figure 5 also shows similar findings where the numerical model curve prediction matched the load-deflection's ascending curve from the test result. The anomaly that was found after the ultimate point resulted from the assumption of the bilinear model of the reinforcing bar. The threshold of the bars' condition when buckled or strain hardened should be included in the analysis to better predict the response after the ultimate point.

Table 3 Summary of lateral load at each level

Level	Lateral load (kN)		Ratio
	Experimental	3D-NLFEA	
Elastic	23.00	27.82	0.827
Post Yielding	56.50	57.80	0.978
Ultimate	70.00	72.61	0.964
Failure	40.00	73.67	0.543
Statistical Evaluation from Elastic to Ultimate Stage			
Mean			0.971
Covariance			1.02 %

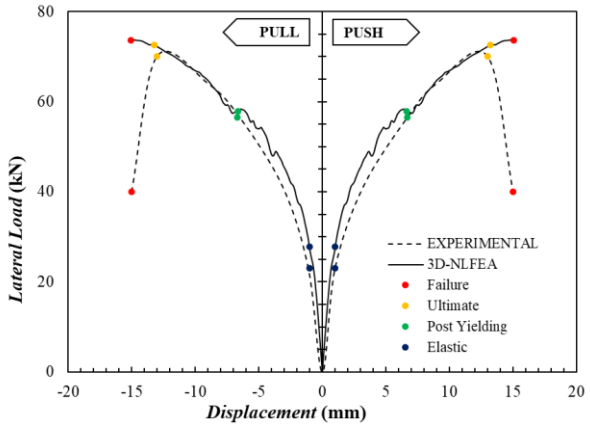

Figure 5 Lateral load-displacement curve comparison

B. MODIFICATION OF THE EXPERIMENTAL MODEL USING HSS REBAR

To study the effect of using the HSS rebar with G100 and G120, the rebar in the verified shear model will be changed from NSS to HSS. The quality of the concrete was set to be like that in [15]. In total, four models are being investigated, which are: the shear wall with the grade 100 HSS rebar, the shear wall with G120 HSS rebar, the shear wall with combination configuration G100 HSS rebar and NSS rebar, and shear wall with combination configuration G120 HSS rebar and NSS rebar.

The material properties of the HSS rebar were obtained from ASTM 1035 [25], [26]. The diameter of the HSS rebar was adjusted accordingly to maintain similar strength of the shear wall. Table 4 shows the material properties of the HSS rebar. It should be noted that the rebar was modeled using an embedded technique and was assumed to have a perfect bond. Figure 6 shows the rebar configuration for the whole shear wall made of the HSS rebar and the shear wall made of the HSS and NSS rebars combined. In Figure 6, the HSS rebar was presented as a red-colored line, while the NSS rebar was presented as a blue-colored line.

Table 4 Tensile properties of HSS

HSS Grade	Diameter (mm)	Yield Strength (kN/mm^2)	Modulus of Elasticity (kN/mm^2)
100	5	0.690	200
120	4.5	0.830	200

The output obtained from the analysis was the horizontal force and the displacement at the top of the shear wall. The collected data was used to analyze the strength and stiffness of the shear wall. The crack pattern was investigated by looking at the strain distribution. The visualization of the result was made possible using the ParaView software. Since the output prepared for the stress in the ParaView was in the form of a stress tensor, a simple two-dimension principal stress equation was used to investigate the principal stress in the shear wall and is:

$$\sigma_{x,y} = \frac{\sigma_x + \sigma_y}{2} \pm \sqrt{\left(\frac{\sigma_x + \sigma_y}{2}\right)^2 + \tau_{xy}^2} \quad (1)$$

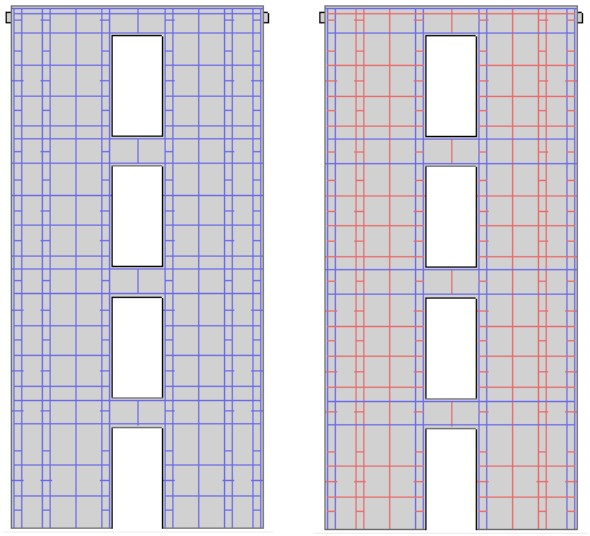

(a) HSS (b) HSS & NSS

Figure 6 HSS and combination bar configuration

ANALYSIS AND DISCUSSIONS

A. STRENGTH OF THE SHEAR WALL

The lateral load and displacement data obtained from 3D-NLFEA were processed further to see the relationship between each model. Figure 7 shows the plotted curves for each modified model (NSS, HSS, and a combination of NSS and HSS). Table 5 summarizes the lateral load capacity for each of the adjusted models.

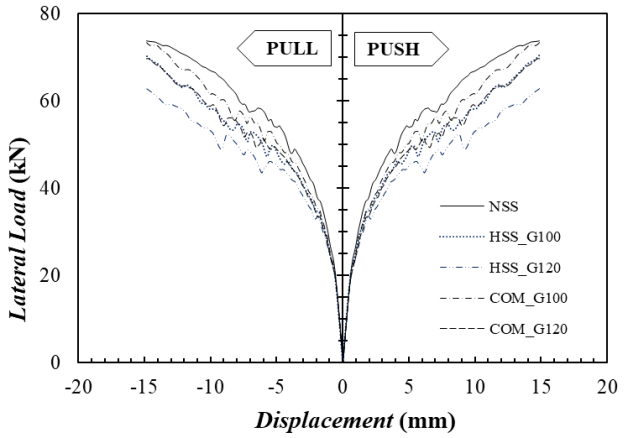

Figure 7 Lateral load-displacement curve of the modified model

From Figure 7, the shear wall with the NSS rebar configuration performs the best in terms of the capacity to resist the lateral load (P_u = 73.79 kN). On the other hand, the shear wall with the G120 HSS rebar configuration has the lowest lateral load capacity (P_u = 62.87 kN). The shear wall with the G100 HSS rebar has a lateral load capacity of 70.45 kN. From the comparisons above, it can be concluded that using HSS rebar reduces the ultimate strength of the shear wall lateral load-carrying capacity. The higher the yield strength of the bar, the lower the shear wall lateral load-carrying capacity. This reduction in capacity can be easily understood as more damage is required to make the rebar yield, thus lowering the stiffness, increasing the deformation, and reducing lateral load-carrying capacity.

As for the shear wall with the combined NSS and HSS, the lateral load carrying capacity for the shear wall with the NSS and G100 HSS rebars is 73.44 kN, while for the shear wall with NSS and G120 HSS rebars is 69.66 kN. From this study, it can also be concluded that combining the NSS and G100 HSS rebar only yields slightly lower capacity than a shear wall made with the NSS rebar only. Therefore, with the reduction in rebar area due to replacement from NSS to HSS, the structural weight can be less and steel congestion at the boundary elements of the shear well can be avoided.

Table 5 Lateral load carrying capacity of the shear wall with different rebar configuration

Bar Configuration	P_u (kN)	Percentage of Reduction (%)
NSS	73.79	
HSS G100	70.45	4.53
HSS G120	62.87	14.80
Combination NSS (57,3%) + HSS G100 (42,7%)	73.44	0.48
Combination NSS (57,3%) + HSS G120 (42,7%)	69.66	5.61

B. CRACK PATTERN OF THE SHEAR WALL

The crack characteristics such as length, width, and distance are important indicators of the mechanical properties of reinforced concrete structures [28]. The crack pattern is obtained by investigating the strain localization in the model. The crack patterns that are reviewed are cracks that occur because of maximum pull or push loads. Figure 8 shows the crack pattern for each of the modified models.

Based on the result in figure 8, when viewed from the configuration of the reinforcement used, the cracks in the shear wall with the NSS configuration that occur are mostly centered on the base of the wall, where these tend to be flexural (horizontal) cracks, but shear cracks also occur. Meanwhile, for shear walls with HSS reinforcement systems or combinations, the cracks are evenly distributed, tending to be shear cracks (diagonal). The greatest damage to shear walls occurs in structures with the NSS configuration. Meanwhile, the smallest damage occurred on the structure with the HSS configuration. For combination configurations, it is in between. So, shear walls with the same ratio of reinforcement and reinforcement capacity, the higher the quality of the reinforcement used, the less damage to the structure, while

the lower the quality of the reinforcement used, the greater the damage to the structure.

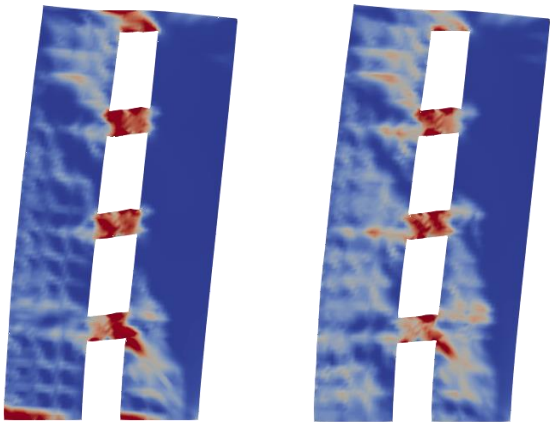

(a) NSS (b) HSS G100

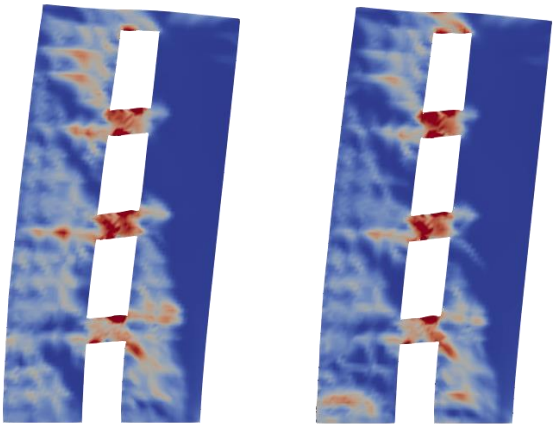

(c) HSS G120 (d) NSS + HSS G100

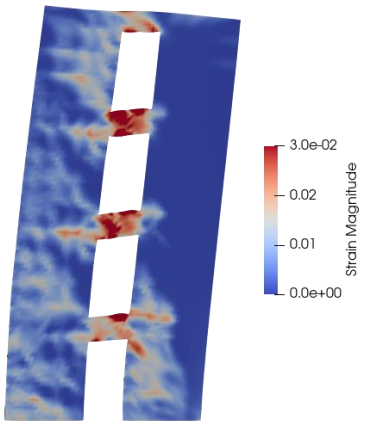

(e) NSS + HSS G120

Figure 8 Crack pattern (strain localization)

C. PRINCIPAL STRESS IN THE CONCRETE

The maximum compressive stress in the concrete is obtained from the principal stress in the element. The shear wall with NSS configuration has 31.76 MPa. While the shear wall with the G100 HSS rebar and the G120 HSS resulted in 32.16 MPa and 30.01 MPa of compressive stress, respectively. For a shear wall with a combined NSS and G100 HSS, the maximum compressive stress is 34.40 while the other one with G120 HSS has a value of 34.72 MPa. The result of the principal stress was shown in Table 7. From this section, it can be concluded that as the strength of the bar increases, the compressive stress in the shear wall concrete was reduced and vice versa.

Table 6 Maximum principal stress in the shear wall concrete

Bar Configuration	Principal Stress (*MPa*)	Percentage of Reduction (%)
NSS	31.76	
HSS G100	32.16	+1.3
HSS G120	30.01	-5.5
Combination G100	34.40	+8.3
Combination G120	34.72	+9.3

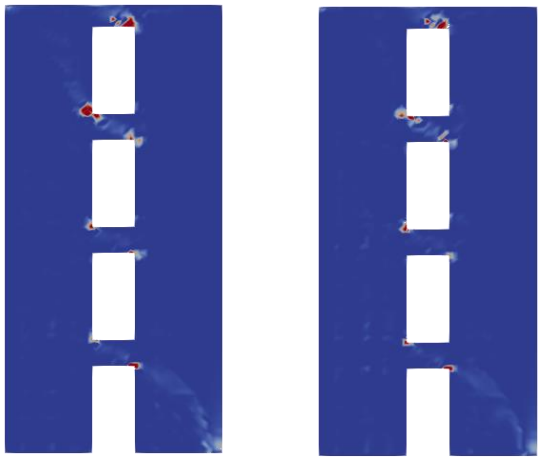

(a) NSS (b) HSS G100

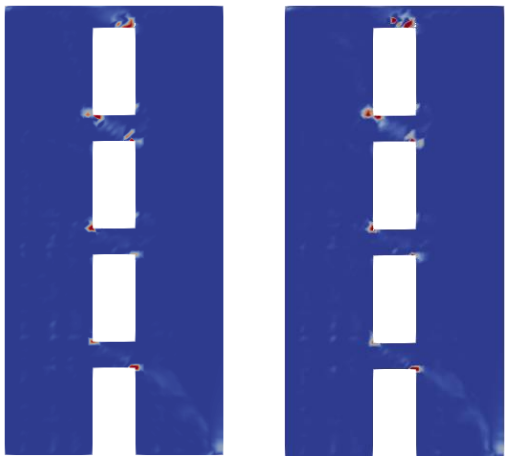

(c) HSS G120 (d) NSS + HSS G100

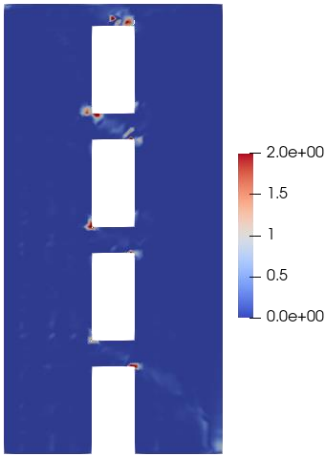

(e) NSS + HSS G120

Figure 9 Hardening parameter

D. HARDENING PARAMETER IN THE CONCRETE

Figure 9 shows the hardening parameter in the concrete. In Figure 9, the legend shows the hardening parameter with a value ranging from 0.0 to 2.0. An element that has a hardening parameter value greater than 1.0 indicates that the concrete in that element is at the softening phase while if the value of hardening parameter was less than 1.0, the concrete is at the hardening phase. As shown in Figure 9, the hardening parameter contour that has values greater than unity was localized at the corner openings which was expected.

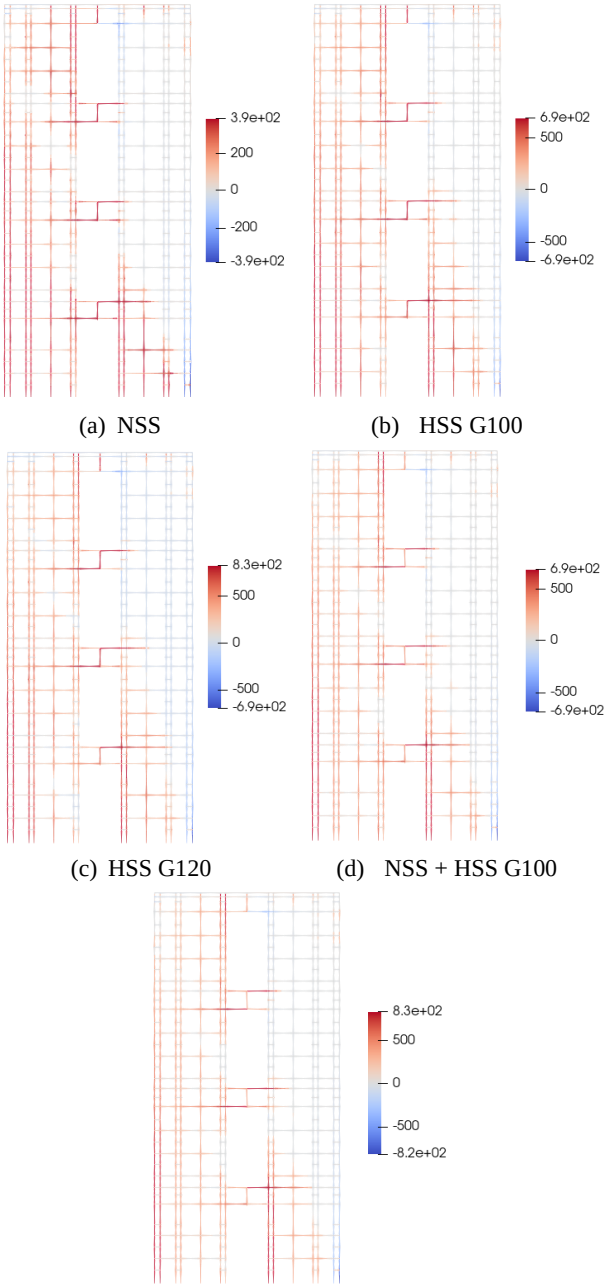

(a) NSS (b) HSS G100

(c) HSS G120 (d) NSS + HSS G100

(e) NSS + HSS G120

Figure 10 Stress distribution of rebar

E. STRESS DISTRIBUTION ON THE REBAR

Figure 9 shows the stress distribution in the reinforcing bar for each modified model. From Figure 9, the legend was adjusted such that the maximum and the minimum values show the yield limit for compression and tension conditions. Hence, it can be seen that the highest tension bar is located at the left part of the shear wall, which falls in the tension region. Another interesting finding is that the bar stresses in the coupling beam also show tension in the top right and the bottom left rebar, as shown in Figure 9. The bar condition at that location can be seen to have yielded.

CONCLUSIONS

This paper presented the nonlinear behavior of RC shear walls with regular openings influenced by high-strength steel using numerical simulation with a 3D-NLFEA finite element package. The 3D-NLFEA finite element package can reasonably predict the behavior of the shear wall with large openings up to the ultimate point. A discrepancy between the numerical model and the test result was found in the failure point because of using a bilinear stress-strain model for the rebar and not considering the buckling of the bar during the analysis.

The parametric studies by replacing the use of the NSS rebar with the HSS rebar showed that by utilizing the HSS rebar with the same reinforcement capacity and ratio is a decrease in the ability to accept lateral loads by 12.22%. In addition, the damage to the shear wall structure is smaller than that of the NSS configuration. For stress distribution with the use of HSS, the stress that occurs is small, the distribution of compressive stress is small and the area of concrete that is experiencing crushing is also small. Then for the HSS configuration, the reinforcement has not melted, while for the NSS configuration and the combination of many reinforcements that have yielded. The crack patterns that occur on shear walls with NSS configuration are flexural and shear cracks, while the crack patterns for structures with HSS configuration or combination (NSS+HSS) are shear cracks. Most of the reinforcement that experiences yielding is the reinforcement in the area below the shear wall structure and the reinforcement that functions as a concealed column.

REFERENCES

[1] A. Wibowo, B. Kafle, A. M. Kermani, N. T. K. Lam, J. L. Wilson, and E. F. Gad, “Damage in the 2008 China earthquake,” Procs. of Australian Earthquake Engineering Society Conference, 2008, pp. 1–8.

[2] C. Popescu, G. Sas, T. Blanksvärd, and B. Täljsten, “Concrete Walls Weakened by Openings as Compression Members: A review,” Engineering Structures, vol. 89, pp. 172–190, 2015, doi: 10.1016/j.engstruct.2015.02.006.

[3] A. M. Fares, “The impact of RC shear wall openings at the lateral stiffness of the cantilever shear walls,” Research on Engineering Structures and Materials, vol. 7, no. 1, pp. 52–63, 2021, doi: 10.17515/resm2020.208st0816.

[4] S. S. Chaudhary, and S. R. Parekar, “Stress distribution of different shapes of opening in shear wall,” SSRN Electronic Journal, vol. 5, no. 8, pp. 8–11, 2019, doi: 10.2139/ssrn.3443674.

[5] E. Montazeri, N. Panahshahi, and B. Cross, “Nonlinear finite element analysis of reinforced

concrete shear walls with staggered openings under seismic loads," Structures Congress 2018, pp. 65–80, 2018.

[6] M. S. Huq, E. A. Burgos, R. D. Lequesne, and A. Lepage, "High-strength steel bars in t-shaped concrete walls," in 11th National Conference on Earthquake Engineering 2018, NCEE 2018: Integrating Science, Engineering, and Policy, 2018, vol. 12, no. 128, pp. 7417–7427.

[7] H. Ma, H. M. Zhang, and Y. Q. Zhai, "Experimental study on seismic performance of RC shear wall with high-strength rebars," in International Efforts in Lifeline Earthquake Engineering - Proceedings of the 6th China-Japan-US Trilateral Symposium on Lifeline Earthquake Engineering, 2014, no. 2012, pp. 505–512, doi: 10.1061/9780784413234.065.

[8] J.-Y. Lee, M. Haroon, D. Shin, and S.-W. Kim, "Shear and torsional design of reinforced concrete members with high-strength reinforcement," Journal of Structural Engineering, vol. 147, no. 2, p. 04020327, 2021, doi: 10.1061/(asce)st.1943-541x.0002887.

[9] A. C. Institute, Building code (ACI 318-19) and commentary on building code requirements for structural concrete (ACI 318R-19)(Farmington Hills, MI). 2019

[10] I. Imran, and R. Simatupang, "Pengaruh jenis baja tulangan terhadap perilaku plastifikasi elemen struktur SRPMK," Jurnal Teknik Sipil, vol. 6, no. 1, pp. 32–45, 2019, doi: 10.28932/jts.v6i1.1325.

[11] R. Bjorhovde, "Performance and design issues for high strength steel in structures," Advances in Structural Engineering, vol. 13, no. 3, pp. 403–411, 2010, doi: 10.1260/1369-4332.13.3.403.

[12] N. I. S. Technology, Use of high-strength reinforcement in earthquake-resistant concrete structures. NIST GCR 14-917-30 Report, prepared by the NEHRP Consultants Joint Venture, a partnership of the Applied Technology Council and the Consortium of Universities for Research in Earthquake Engineering, 2014.

[13] A. S. T. Materials, ASTM A706 - Standard specification for low-alloy steel deformed and plain bars for concrete, 2016 doi: 10.1520/A0706.

[14] A. S. T. Materials, ASTM A615/A615M - Standard specification for deformed and plain billet-steel bars for concrete, 1999 doi: 10.1520/A0615.

[15] M. Marius, "Seismic behaviour of reinforced concrete shear walls with regular and staggered openings after the strong earthquakes between 2009 and 2011," Engineering Failure Analysis, vol. 34, pp. 537–565, 2013, doi: 10.1016/j.engfailanal.2013.05.014.

[16] B. Piscesa, M. M. Attard, A. K. Samani, and S. Tangaramvong, "Plasticity constitutive model for stress-strain relationship of confined concrete," ACI Structural Journal, vol. 114, no. 2, pp. 361–371, Mar. 2017, doi: 10.14359/51689428.

[17] A. K. Samani, and M. M. Attard, "A stress-strain model for uniaxial and confined concrete under compression," Engineering Structures, vol. 41, pp. 335–349, 2012, doi: 10.1016/j.engstruct.2012.03.027.

[18] B. Piscesa, Modeling confined concrete using plasticity formulation, UNSW Sydney, 2018.

[19] M. M. Attard and S. Setunge, "Stress-strain relationship of confined and unconfined concrete," ACI Materials Journals, vol. 93, no. 5, pp. 432–442, 1996, doi: 10.14359/9847.

[20] B. Piscesa, M. M. Attard, D. Prasetya, and A. K. Samani, "Modeling cover spalling behavior in high strength reinforced concrete columns using a plasticity-fracture model," Engineering Structures, vol. 196, 2019, doi: 10.1016/j.engstruct.2019.109336.

[21] B. Piscesa, M. M. Attard, and A. K. Samani, "A lateral strain plasticity model for FRP confined concrete," Composite Structures, vol. 158, pp. 160–174, 2016.

[22] B. Piscesa, M. M. Attard, and A. K. Samani, "Three-dimensional finite element analysis of circular reinforced concrete column confined with FRP using plasticity model," Procedia Engineering, vol. 171, pp. 847–856, 2017.

[23] B. Piscesa, M. M. Attard, and A. K. Samani, "A lateral strain plasticity model for FRP confined concrete," Composite Structures, vol. 158, 2016, doi: 10.1016/j.compstruct.2016.09.028.

[24] A. A. Ulfa, B. Piscesa, M. M. Attard, F. Faimun, and P. Aji, "Parametric studies on the ductility of axial loaded square reinforced concrete column made of normal-strength concrete (NSC) and high-strength steel confining rebar (HSSCR) with various ties configuration," E3S Web of Conferences, 2020, vol. 156, pp. 0–6, doi: 10.1051/e3sconf/202015603002.

[25] A. S. T. Materials, ASTM A1035/A1035M - 09 : Standard specification for deformed and plain low-alloy steel bars for concrete, 2010 doi: 10.1520/A1035.

[26] A. C. I. Committe 439, ACI 439.6R-19 : Guide for the use of ASTM A 1035/ A 1035M type CS grade 100 (690) steel bars for structural concrete. (Farmington Hills: American Concrete Institute), 2019.

[27] T. J. Sullivan, G. M. Calvi, and M. J. N. Priestley, "Initial stiffness versus secant stiffness in displacement based design," 13th World Conference of Earthquake Engineering (WCEE), 2004, vol. 65, no. 2888, pp. 581–626.

[28] T. C. Hutchinson, and T. Wang, "Evaluation of crack spacing in reinforced concrete concrete shear walls," Journal of Structural Engineering, vol. 135, no. 5 May, pp. 499–508, 2009, doi: 10.1061/(ASCE)0733-9445(2009)135:5(499).